Atmos. Chem. Phys. Discuss., 9, 15867–15889, 2009
www.atmos-chem-phys-discuss.net/9/15867/2009/

Atmospheric Chemistry and Physics Discussions

This discussion paper is/has been under review for the journal *Atmospheric Chemistry and Physics (ACP)*. Please refer to the corresponding final paper in *ACP* if available.

Measuring condensation sink and ion sink of atmospheric aerosols with the electrical low pressure impactor (ELPI)

H. Kuuluvainen[1], J. Kannosto[1], A. Virtanen[1], J. M. Mäkelä[1], M. Kulmala[2], P. Aalto[2], and J. Keskinen[1]

[1]Aerosol Physics Laboratory, Department of Physics, Tampere University of Technology, P.O. Box 692, 33101 Tampere, Finland
[2]Department of Physical Sciences, Division of Atmospheric Sciences, University of Helsinki, P.O. Box 64, 00014 University of Helsinki, Finland

Received: 12 May 2009 – Accepted: 9 July 2009 – Published: 27 July 2009

Correspondence to: J. Keskinen (jorma.keskinen@tut.fi)

Published by Copernicus Publications on behalf of the European Geosciences Union.

Abstract

We investigate the suitability of ELPI for condensation sink and ion sink measurements. The aim is to find the simple calibration factors by which the measured ELPI currents can be converted to condensation or ion sinks. The calibration is based on DMPS and ELPI measurements within the period 15–25 May 2005 at a boreal forest site in Southern Finland. The values of condensation sink and ion sink were calculated from the DMPS size distributions using their theoretical definitions. After that the values were compared to theoretical and measured ELPI current, and calibration factors were specified. For condensation sink the calibration factor was found to be 7.27 E-06 s^{-1} fA^{-1} and for ion sink 7.33 E-06 s^{-1} fA^{-1}. Simply by multiplying the total current of the outdoor ELPI by these factors, the values of condensation sink and ion sink can be measured.

1 Introduction

Aerosol particles are omnipresent in the Earth's atmosphere and involved in many atmospheric prosecces affecting the global climate system. Direct effects, including light scattering and absorption, are physically rather simple and well-known phenomena, as against indirect effects related to cloud formation are more complicated (Lohmann and Feichter, 2005; Haywood and Shine, 1995). Uncertainty in these indirect effects has lately motivated us to investigate especially some basic phenomena of atmospheric aerosols: the formation of new particles and their subsequent growth process (Kulmala and Kerminen, 2008; Kulmala et al., 2004).

The growth process of atmospheric aerosol particles is mainly condensational in the presence of condensable species, e.g. water and sulphuric acid with a low vapour pressure. In this respect, the concept of *condensation sink* (Pirjola et al., 1999; Kulmala et al., 2001) is useful. In addition to the condensable species, there are always some ions present in the air. When ions attach onto the particles, the concept of *ion sink* becomes relevant. Because in these processes aerosol particles interact with molecules

ACPD

9, 15867–15889, 2009

or ions through their surface, condensation sink and ion sink are also related to surface metrics called *Fuchs surface* (Pandis et al., 1991) and *active surface* (Siegmann and Siegmann, 2000).

The surface-related quantities can be calculated from size distribution and concentration measured with (e.g.) Differential Mobility Particle Sizer (DMPS) or Scanning Mobility Particle Sizer (SMPS). However, they can also be measured more directly with intruments that mimic the size dependence of these quantities (Shin et al., 2007; Bukowiecki et al., 2002; Woo et al., 2001; Keskinen et al., 1991; Gäggeler et al., 1989). One of the most promising instruments for the real-time measurements of these quantities is a diffusion charger. What happens in a diffusion charger when ions attach onto the particles is intimately related to natural condensation or ion attachment in the atmosphere. Accordingly, it has been shown that the output signal of the diffusion charger is almost directly proportional to many surface related quantities (Fissan et al., 2006; Ntziachristos et al., 2004). Recently, Ntziachristos et al. (2007) applied the Nanoparticle Surface Area Monitor (NSAM, TSI, Inc.) for the measurement of particle surface concentrations of urban and traffic aerosols.

In this study we focus on the electrical low pressure impactor (ELPI), developed by Keskinen et al. (1992). In the ELPI, the sample flow passes through a diffusion charger into a cascade impactor. Each impactor stage is connected to a sensitive current-to-voltage amplifier (electrometer). In normal operation, each electrometer signal is treated separately to calculate size distribution. However, the instrument can also be treated as a diffusion charger simply by summing up all the electrometer signals. We first treat the theoretical instrument response to condensation sink and ion sink. We then check this with experimental data and calculate calibration factors for both condensation sink and ion sink measurement.

2 Attachment rates

If aerosol particles are surrounded by atoms, molecules or ions that attach to the particles, the concentration of the present species n obeys the first order differential equation

$$\frac{\mathrm{d}n}{\mathrm{d}t} = -Xn, \tag{1}$$

where X is the attachment rate of the species onto the particles. For a polydispersed aerosol the attachment rate is obtained by integrating a particle size dependent attachment rate factor $A_X(d_p)$ over the aerosol size distribution $\mathcal{N}(d_p)$:

$$X = \int A_X(d_p)\mathcal{N}(d_p)\,\mathrm{d}d_p\,. \tag{2}$$

These expressions were originally used for the attachment of airborne radioactive species onto aerosol particles (e.g. Porstendörfer and Mercer, 1978) but they are quite generic. We apply them to condensing species (marking X=CS and A_X=A_{CS}) and to attaching ions (marking X=IonS and A_X=A_{IonS}).

2.1 Condensation sink

For condensing atoms and molecules, we name the rate quantity of Eq. (1) as condensation sink (CS) and the corresponding attachment rate factor as condensation sink factor $A_{\mathrm{CS}}(d_p)$. The latter is defined as:

$$A_{\mathrm{CS}}(d_p) = 2\pi d_p D_m \beta(d_p), \tag{3}$$

where d_p is the particle diameter, D_m the diffusion coefficent of the gas molecules, and β the Fuchs correction factor. As a correction factor we use the Fuchs and Sutugin (1971) formula in the form of

$$\beta = \frac{1 + Kn}{1 + \left(\frac{4}{3\alpha} + 0.377\right) Kn + \frac{4}{3\alpha} Kn^2}, \tag{4}$$

ACPD
9, 15867–15889, 2009

where Kn is the relation of the particle diameter and the mean free path of the gas λ_m, called Knudsen number. The particle size dependence of the condensation sink factor is shown in Fig. 1.

According to the definition, the condensation sink of the aerosol depends on the properties of the molecules or the atoms, i.e. the diffusion coefficient and the mean free path. In this paper we use the properties of sulfuric acid because it has been identified as a key component in atmospheric aerosol formation and growth (Riipinen et al., 2007). The diffusion coefficient of vapour molecules in the air is calcuated as (Poling et al., 2000)

$$D_{\mathrm{vap}} = 0.00143 \cdot T^{1.75} \frac{\sqrt{M_{\mathrm{air}}^{-1} + M_{\mathrm{vap}}^{-1}}}{P(D_{x,\mathrm{air}}^{1/3} + D_{x,\mathrm{vap}}^{1/3})^2}, \quad (5)$$

where P is the air pressure, M the molar mass and D_x the diffusion volume, which is calculated from the table of atomic diffusion volumes gathered by Poling et al. (2000). The values are found to be $D_{x,\mathrm{air}}$=19.7 and $D_{x,\mathrm{vap}}$=51.66 for the sulfuric acid molecules. Thus we get the diffusion coefficient of the sulfuric acid. The relation between the diffusion coefficient and the mean free path is known to be $\lambda_m = 3\overline{c}_m / D_m$, where $\overline{c}_m$ is the mean thermal velocity of the molecules. Due to the temperature-dependent molecule properties, we have now the condensation sink dependent on temperature. The molecule properties are also dependent on the air pressure, but in this paper it is kept invariant.

2.2 Ion sink

For airborne ions, we name the rate quantity of Eq. (1) as ion sink (IonS) and the corresponding attachment rate factor as ions sink factor $A_{\mathrm{IonS}}(d_p)$. The ion sink factor is defined as:

$$A_{\mathrm{IonS}}(d_p, p) = \int \eta(d_p, p) \Psi(d_p, p)\, \mathrm{d}p\,, \quad (6)$$

ACPD
9, 15867–15889, 2009

where p is the number of elementary units of charge and η is the combination coefficient introduced by Fuchs (1963). The integral is taken over the charge distribution Ψ of the particles. We adopt the notation used by Adachi et al. (1985) for the combination coefficient

$$\eta = \frac{\pi \overline{c}_i \xi \delta^2 \exp\left(\frac{-\phi(\delta)}{k_B T}\right)}{1 + \exp\left(\frac{-\phi(\delta)}{k_B T}\right) \frac{\overline{c}_i \xi \delta^2}{4 D_i a} \int_0^{a/\delta} \exp\left(\frac{\phi(a/x)}{k_B T}\right) \mathrm{d}x}, \quad (7)$$

where $a{=}d_p/2$, $x{=}a/r$ and

$$\delta = \frac{a^3}{\lambda_i^2}\left(\frac{1}{5}\left(1 - \frac{\lambda_i}{a}\right)^5 - \frac{1}{3}\left(1 + \frac{\lambda_i^2}{a^2}\right)\left(1 + \frac{\lambda_i}{a}\right)^3 + \frac{2}{5}\left(1 + \frac{\lambda_i^2}{a^2}\right)^{5/2}\right),$$

$$\phi(r) = \frac{pe^2}{4\pi\varepsilon_0 r} - \frac{\varepsilon_r - 1}{\varepsilon_0 - 1}\frac{e^2}{8\pi\varepsilon_0}\frac{a^3}{r^2(r^2 - a^2)},$$

where r is the distance between ion and particle centre, e the elementary charge, ε_0 the dielectric constant, ε_r the specific dielectric constant, λ_i the mean free path of ions and ξ the striking probability. The size dependence of ion sink factor is shown in Fig. 1.

There are several ways to calculate the ion properties introduced above. We use the following equations (Hoppel and Frick, 1986):

$$D_i = k_B T Z_i / e$$

$$\overline{c}_i = \sqrt{\frac{8 k_B T}{\pi (M_i / N_A)}}$$

ACPD
9, 15867–15889, 2009

$$\lambda_i = \frac{4Z_i}{3e}\sqrt{\frac{8k_BTM_{\text{air}}^2}{\pi(M_i + M_{\text{air}})N_A}},$$

where D_i is the diffusion coefficient, Z_i the electrical mobility, k_B the Boltzmann coefficient, $\bar{c}_i$ the mean thermal velocity, M the molar mass, N_A the Avogadro number and λ_i the mean free path. The electrical mobility of ions is dependent on temperature and pressure. Commonly used notation for the dependence is (Eiceman and Karpas, 2005)

$$Z_i = Z_0 \frac{P}{P_0}\frac{T_0}{T}. \quad (8)$$

In this paper only the temperature dependence is taken into account and the pressure is kept invariant. As the molar mass and as the mobility in temperature T_0=293.15 K we use the values of positive ions measured by Vohra et al. (1969): M_i=0.109 kg/mol and Z_0=1.4×10^{-4} m^{2}s/V.

3 The attachment rates compared to ELPI current

Based on the theoretical definition of ion sink, its proportionality to the diffusion charging of aerosol particles seems to be evident. Although using so-called active surface metric, which is directly proportional to ion sink, Ntziachristos et al. (2004) showed that this quantity correlated with the current signal of the diffusion charger. They also showed that there is a small difference between the active and the so-called Fuchs surface metric, the latter of which is directly proportional to condensation sink.

ELPI response function

The electrical low pressure impactor (ELPI) is an instrument that, by calculating the total current of all impactor stages, provides a real-time current signal of the particles

charged with a diffusion charger. Using the notation of Keskinen et al. (1991) the total current, as an outputsignal of ELPI, can be expressed as

$$I = \int S_N(d_p)\mathcal{N}(d_p)\,\mathrm{d}d_p \tag{9}$$

where $S_N(d_p)$ is defined as a number sensitivity function of the instrument. According to Marjamäki et al. (2000) the number sensitivity function of ELPI is

$$S_N(d_p) = Pn(d_p)eQ, \tag{10}$$

where P is the penetration through the charger, n is the number of single charges per particle and Q is the flowrate through the charger. In our measurements we used an outdoor ELPI, which had a flowrate Q=28.91 l/s. Manufacturer (Dekati Ltd., 2003) gives the number sensitivity function of the outdoor ELPI as:

$$PneQ = \begin{cases} 3.0924 \cdot \frac{Q}{Q_0} \cdot {d_p}^{1.3915}, & d_p \leq 0.0135\ \mu\mathrm{m} \\ 2.0000 \cdot \frac{Q}{Q_0} \cdot {d_p}^{1.2902}, & d_p > 0.0135\ \mu\mathrm{m} \end{cases}, \tag{11}$$

where Q_0=10 l/s and the unit of the quantity $PneQ$ is 1/(fA cm^3). The number sensitivity function compared to the attachment rate factors is shown in Fig. 1.

Measuring an arbitrary quantity $A(d_p)$, the instrument is said to be ideal if $S_N(d_p)$=$KA(d_p)$ and K is a constant. In the non-ideal case the sensitivity function is not directly proportional to $A(d_p)$ and we can define a size dependent quantity

$$K(d_p) = \frac{S_N(d_p)}{A(d_p)}, \tag{12}$$

which is called the response function of the instrument specified by $A(d_p)$. Specifically, we are interested in the response functions specified by the factors A_{CS} and A_{IonS}, defined in Eqs. (3) and (6), respectively (Fig. 2). The only quantity, that actually behaves ideally, is the number sensitivity function itself. However, as could be seen in the Fig. 2, the response function specified by ion sink differs only slightly from the ideal behaviour. The response is near-ideal also in the case of condensation sink.

ACPD
9, 15867–15889, 2009

4 Measurements

The measurements were carried out at the SMEAR II station (Hari and Kulmala, 2005) in Hyytiälä, Southern Finland, between 15 and 25 May 2005. The field station is located in a boreal forest and it represents a typical background area of Finland. Concentration and consistence of the aerosol are highly dependent on wind direction and air mass trajectories. All the well-known modes of atmospheric aerosols are detected.

The period of May was chosen because there were a number of changes in the size distrubution of particles as well as in temperature, and these ten days represent well the round-year average. Examples of the number size distributions and the average distribution are shown in Fig. 3. All the measured distributions during the period are plotted as a function of time in Fig. 7a.

Particle size distributions were measured with DMPS, including two Vienna type DMAs with 10.9 cm and 28 cm tube lengths, CPC 3025 and CPC 3010 (Mäkelä et al., 1997). In addition, there was the outdoor ELPI. The time resolutions of ELPI and DMPS were one and ten minutes, respectively, but the ELPI data was averaged over ten minutes to correspond the DMPS data. ELPI measures particles approximately in the size range 7 nm–6 μm while the DMPS size range is about 3 nm–500 nm. Along with these aerosol particle measurements air temperature was measured continuously during the period.

5 Calibration

At first, the values of condensation sink and ion sink were calculated using the measured DMPS size distributions, the Eqs. (3) and (6), the properties of sulfuric acid molecules and positive ions represented earlier, and the measured temperature. On account of the DMPS time resolution, we had 1440 calculated values per attachment rate altogether.

ACPD
9, 15867–15889, 2009

5.1 Theoretical calibration

By theoretical calibration we mean that the outdoor ELPI is calibrated to measure the attachment rates using only the DMPS data. The ELPI current response corresponding to each DMPS size distribution, also called theoretical ELPI current in this context, is calculated by means of the sensitivity function (11) and the equation

$$I_{\text{theor}} = \int Pn(d_p)eQ \cdot \mathcal{N}(d_p)\,\mathrm{d}d_p\,. \tag{13}$$

It is now possible to plot the attachment rates as a function of the theoretical ELPI current (Fig. 4). Fittings have been made into the set of points with the method of least squares. The fitted curves are straight lines without a constant term, so the only value describing the compatibility of the fit is the slope, which we call the calibration factor Λ. Theoretical calibration factors are shown in Table 1.

The calibration factor is the number, by which the total current of ELPI has to be multiplied to be able to get the value of the attachment rate. This is a very simple method to measure condensation sink or ion sink and it provides much better time resolution compared to DMPS measurements.

5.2 Calibration using measured ELPI current

Instead of the theoretical ELPI current, measured ELPI current can also be used. There are both advantages and disadvantages in working with the measured current. For ELPI it is definitely more realistic and it takes into account all the losses and characteristics of the instrument affecting the output signal. On the other hand, if there, for some reason, is a difference between the total concentration of the sample measured by DMPS and ELPI, it will have a direct effect on the calibration factor.

The attachment rates as a function of the measured ELPI current are shown in Fig. 5 and the corresponding calibration factors in Table 2. Note that the deviation is more pronounced in this case than in the theoretical case and the values of the calibration factors are slightly different.

5.3 Comparison

We have now two sets of calibration factors, some of them based on solely the DMPS data and the others based on the data from both the instruments. The difference between the output signals of the instruments can be compared by plotting the theoretical ELPI current as a function of the measured ELPI current (Fig. 6). The currents are directly proportional to each other with a correlation of 0.909. For comparison, Ntziachristos et al. (2007) calculated the correlations of the NSAM output and the SMPS based teoretical output. They found correlations of 0.94 and 0.64 for urban and fresh traffic aerosols, repectively. Our result confirms the method of calculating theoretical current from the DMPS data as reasonable. However, the slope of the fitting is 0.885, which means there is a constant factor between the output signals of the instruments. This constant factor is the same as between the calibration factors.

To show the relevance of the method in practice, we have plotted the values of condensation sink and ion sink as function of time in Fig. 7. Both the values calculated from DMPS and the values calculated from the ELPI current are shown. In this figure, we have used the calibration factors based on the measured ELPI current to make the values comparable. The agreement between the two methods is very good.

6 Summary and conclusions

We have shown that ELPI is an instrument able to measure condensation sink and ion sink of atmospheric aerosol particles. The characterization of particle formation and growth processes has recently been a key to understand indirect climate effects of the atmospheric aerosol. In this respect, need for a simple real-time measuring instrument of the surface-related quantities connected to these processes seems to be growing.

We made calibrations based on the DMPS and ELPI data measured in a boreal forest environment. There was a slight difference, about 10%, between the theoretical calibration factors and the calibration factors based on the measured ELPI current.

ACPD
9, 15867–15889, 2009

Could the difference between the size ranges of ELPI (7 nm–6 μm) and DMPS (3 nm–500 nm) be the reason for this? In fact, it could be a part of the explanation, but it does not account for the whole difference because small particles inflict such a minimal current and there are very few particles in the size range 500 nm–6 μm. The relative difference between the measured current and the current corrected with the size range and the diffusion losses was checked to be under 4%. An error in the sensitivity function of the outdoor ELPI may also be a cause for the difference. Another explanation is that there is an error in the total concentration of the sample measured by ELPI or DMPS caused for example by an error in the flow rate. With only one major flow, the ELPI is not very prone to errors in the total concentration. In this respect, DMPS may be more vulnerable. Therefore, we favour the theoretical calibration factors, which assume that ELPI operates theoretically correct, and the DMPS total concentration does not shift the result.

Finally, we establish the universal calibration factors: 7.27 E-06 s^{-1} fA^{-1} for condensation sink and 7.33 E-06 s^{-1} fA^{-1} for ion sink. By multiplying the total current of the outdoor ELPI by these factors the values of the attachment rates can be measured. This is a very simple method and it brings all the advantages of ELPI to the measurements of the attachment rates.

References

Adachi, M., Kousaka, Y., and Okuyama, K.: Unipolar and bipolar diffusion charging of ultrafine aerosol particles, J. Aerosol Sci., 16, 109–123, 1985. 15872

Bukowiecki, N., Kittelson, D. B., Watts, W. F., Burtscher, H., Weingartner, E., and Baltensperger, U.: Real-timecharacterization of ultrafine and accumulation mode particles in ambient combustion aerosols, J. Aerosol Sci., 33, 1139–1154, 2002. 15869

Dekati Ltd.: ELPI charging efficiencies, www.dekati.fi, 2003. 15874

Eiceman, G. A. and Karpas, Z.: Ion Mobility Spectrometry, CRC Press Taylor & Francis, Boca Raton, 2. edn., 2005. 15873

Fissan, H., Trampe, A., Neunman, S., Pui, D. Y. H., and Shin, W. G.: Rationale and principle of an instrument measuring lung deposition area, J. Nanopart. Res., 9, 53–59, 2006. 15869
Fuchs, N. A.: On the stationary charge distribution on aerosol particles in a bipolar ionic atmosphere, Geofisca Purae Applicata, 56, 185–193, 1963. 15872
Fuchs, N. A. and Sutugin, A. G.: High-dispersed aerosols, in: Current Aerosol Research, edited by: Hidy, G. M. and Brock, J., Pergamon, Oxford, 1–60, 1971. 15870
Gäggeler, H. W., Baltensperger, U., and Emmenegger, M.: The epiphanometer, a new device for continuous aerosol monitoring, J. Aerosol Sci., 20, 557–564, 1989. 15869
Hari, P. and Kulmala, M.: Station for Measuring EcosystemAtmosphere Relations (SMEAR II), Boreal Environ. Res., 10, 315–322, 2005. 15875
Haywood, J. M. and Shine, K. P.: The effect of anthropogenic sulfate and soot aerosol on the clear sky planetary radiation budget, Geophys. Res. Lett., 22, 603-606, 1995. 15868
Hoppel, W. A. and Frick, G. M.: Ion-aerosol attachment coefficients and the steady-state charge distribution on aerosols in a bipolar ion environment, Aerosol Sci. Tech., 5, 1–21, 1986. 15872
Keskinen, J., Lehtimäki, M., and Graeffe, G.: Radon decay product attachment rates in dwellings, J. Aerosol Sci., 22, 765-771, 1991. 15869, 15874
Keskinen, J., Pietarinen, K., and Lehtimäki, M.: Electrical low pressure impactor, J. Aerosol Sci., 23, 353–360, 1992. 15869
Kulmala, M. and Kerminen, V.-M.: On the formation and growth of atmospheric nanoparticles, Atmos. Res., 90, 132–150, 2008. 15868
Kulmala, M., Dal Maso, M., Mäkela, J. M., Pirjola, L., Väkevä, M., Aalto, P., Miikkulainen, P., Hämeri, K., and O'Dowd, C. D.: On the formation, growth and composition of nucleation mode particles, Tellus B, 53, 479–490, 2001. 15868
Kulmala, M., Vehkamäki, H., Petäjä, T., Dal Maso, M., Lauri, A., Kerminen, V.-M., Birmili, W., and McMurry, P. H.: Formation and growth rates of ultrafine atmospheric particles: A review of observations, J. Aerosol Sci., 35, 143–176, 2004. 15868
Lohmann, U. and Feichter, J.: Global indirect aerosol effects: a review, Atmos. Chem. Phys., 5, 715–737, 2005, http://www.atmos-chem-phys.net/5/715/2005/. 15868
Mäkelä, J. M., Aalto, P., Jokinen, V., Pohja, T., Nissinen, A., Palmroth, S., Markkanen, T., Seitsonen, K., Lihavainen, H., and Kulmala, M.: Observations of ultrafine aerosol particle formation and growth in boreal forest, Geophys. Res. Lett., 24, 1219–1222, 1997. 15875
Marjamäki, M., Keskinen, J., Chen, D. R., and Pui, D. Y. H.: Performance evaluation of the

electrical low-pressure impactor (ELPI), J. Aerosol Sci., 31, 249–261, 2000. 15874
Ntziachristos, L., Giechaskiela, B., Ristimäki, J., and Keskinen, J.: Use of a corona charger for the characterisation of automotive exhaust aerosol, J. Aerosol Sci., 35, 943–963, 2004. 15869, 15873
Ntziachristos, L., Polidori, A., Phuleria, H., Geller, M. D., and Sioutas, C.: Application of a diffusion charger for the measurement of particle surface area concentration in different environments, Aerosol Sci. Tech., 41, 571–580, 2007. 15869, 15877
Pandis, S. N., Baltensperger, U., Wolfenbarger, J. K., and Seinfeld, J. H.: Inversion of aerosol data from the epiphaniometer, J. Aerosol Sci., 22, 417–428, 1991. 15869
Pirjola, L., Kulmala, M., Wilck, M., Bischoff, A., Stratmann, F., and Otto, E.: Formation of sulphuric acid aerosols and cloud condensation nuclei: an expression for significant nucleation and model comparison, J. Aerosol Sci., 30, 1079–1094, 1999. 15868
Poling, B. E., Prausnitz, J. M., and O'Connel, J. P.: The Properties of Gases and Liquids, McGraw-Hill, 2000. 15871
Porstendörfer, J. and Mercer, T. T.: Adsorption propability of atoms and ions on particle surfaces in submicrometer size range, J. Aerosol Sci., 9, 469–474, 1978. 15870
Riipinen, I., Sihto, S.-L., Kulmala, M., Arnold, F., Dal Maso, M., Birmili, W., Saarnio, K., Teinilä, K., Kerminen, V.-M., Laaksonen, A., and Lehtinen, K. E. J.: Connections between atmospheric sulphuric acid and new particle formation during QUEST III–IV campaigns in Heidelberg and Hyytiälä, Atmos. Chem. Phys., 7, 1899–1914, 2007, http://www.atmos-chem-phys.net/7/1899/2007/. 15871
Shin, W. G., Pui, D. Y. H., Fissan, H., Neumann, S., and Trampe, A.: Calibration and numerical simulation of Nanoparticle Surface Area Monitor (TSI Model 3550 NSAM), J. Nanopart. Res., 9, 61–69, 2007. 15869
Siegmann, K. and Siegmann, H. C.: Fast and reliable "in situ" evaluation of particles and their surfaces with special reference to diesel exhaust, Tech. Rep. 2000-01-1995, SAE, 2000. 15869
Vohra, K. G., Subba Ramu, M. C., and Vasudevan, K. N.: Nucleation of Water Cluster Ions, reports Bhabba Atomic Research Centre, Bombay, 1969. 15873
Woo, K.-S., Chen, D.-R., Pui, D. Y. H., and Wilson, W. E.: Use of continuous measurements of integral aerosol parameters to estimate particle surface area, Aerosol Sci. Tech., 34, 57–65, 2001. 15869

Table 1. Theoretical calibration factors Λ with 95% confidence bounds, the correlation of the fitting and the root mean square error describing the final error of the measured attachment rate.

		IonS	CS
Λ	($s^{-1}\,fA^{-1}$)	7.33 E-06	7.27 E-06
correlation	(–)	0.994	0.970
root mean square error	(s^{-1})	2.77 E-04	7.03 E-04
95% confidence interval	($s^{-1}\,fA^{-1}$)	[7.31 E-06; 7.34 E-06]	[7.23-06; 7.31 E-06]

Table 2. These calibration factors Λ have been calculated by comparing the measured ELPI current and the attachment rates calculated from the DMPS data. Statistical numbers describe the error of the fitting.

		IonS	CS
Λ	(s^{-1} fA^{-1})	6.49 E-06	6.43 E-06
correlation	(–)	0.897	0.894
root mean square error	(s^{-1})	1.146-03	1.33 E-03
95% confidence interval	(s^{-1} fA^{-1})	[6.42 E-06; 6.55 E-06]	[6.36 E-06; 6.50 E-06]

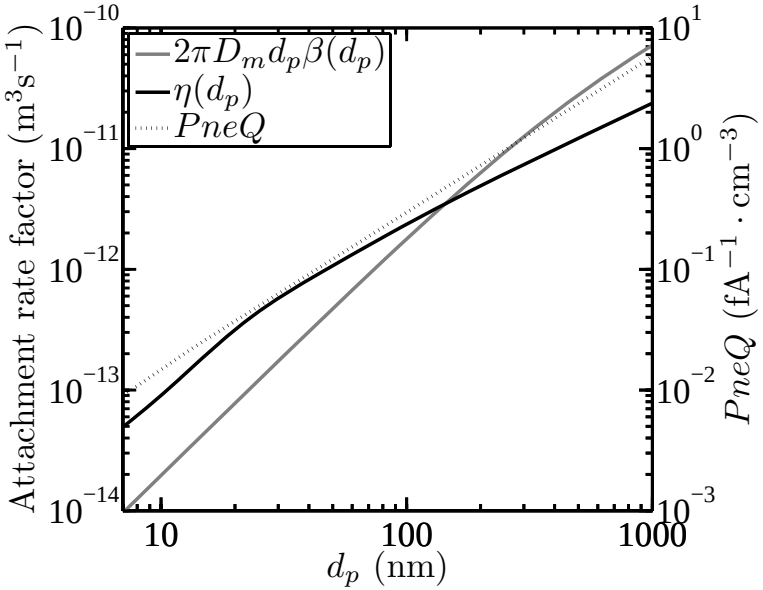

Fig. 1. The particle size dependence of the attachment rate factors for condensation sink ($2\pi D_m d_p \beta(d_p)$) and ion sink ($\eta(d_p)$). The number sensitivity function of the outdoor ELPI (*PneQ*) shown on secondary vertical axis.

ACPD
9, 15867–15889, 2009

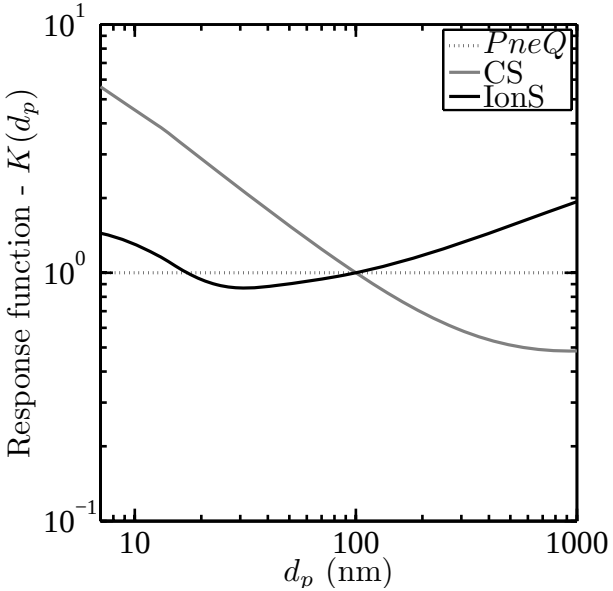

Fig. 2. Response functions of the ELPI total current signal for the ELPI sensitivity function (*PneQ*), for the condensation sink (CS), and for the ion sink (IonS). The functions are normalized at 100 nm.

ACPD
9, 15867–15889, 2009

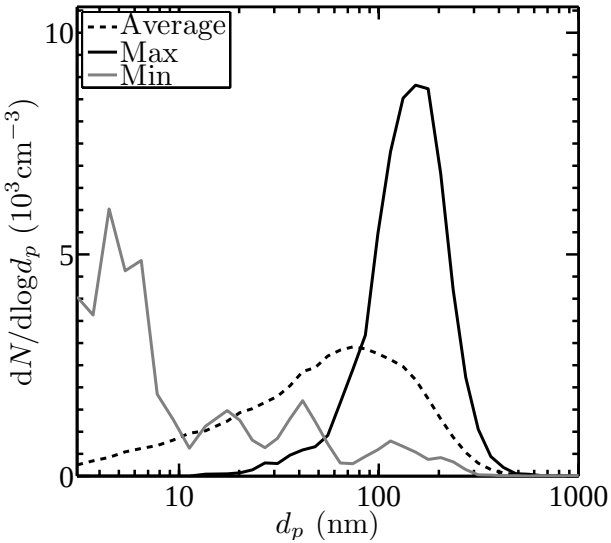

Fig. 3. Examples of the number size distributions measured with DMPS at Hyytiälä in May 2005. *Min* means the distribution with the lowest GMD and *Max* the distribution with the greatest GMD. *Average* is an artificial distribution including the mean values of each DMPS channel in this data.

ACPD
9, 15867–15889, 2009

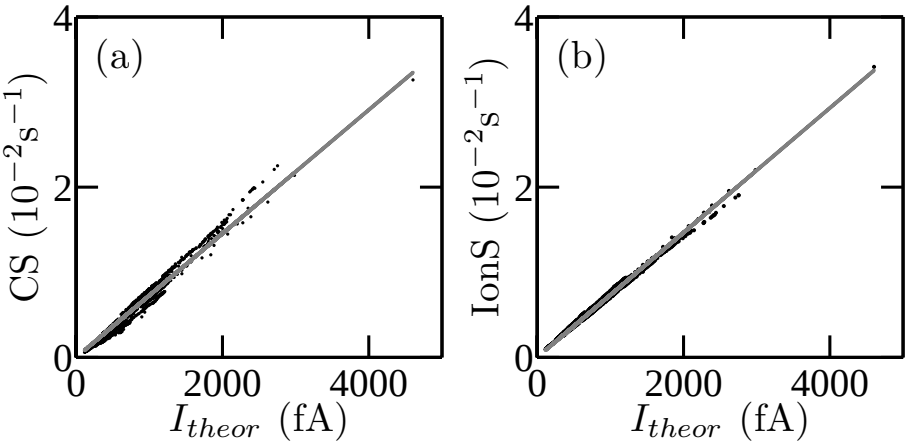

Fig. 4. The values of **(a)** condensation sink and **(b)** ion sink calculated from the DMPS size distributions as a function of the theoretical ELPI current, which is also calculated from the DMPS data using the number sensitivity function.

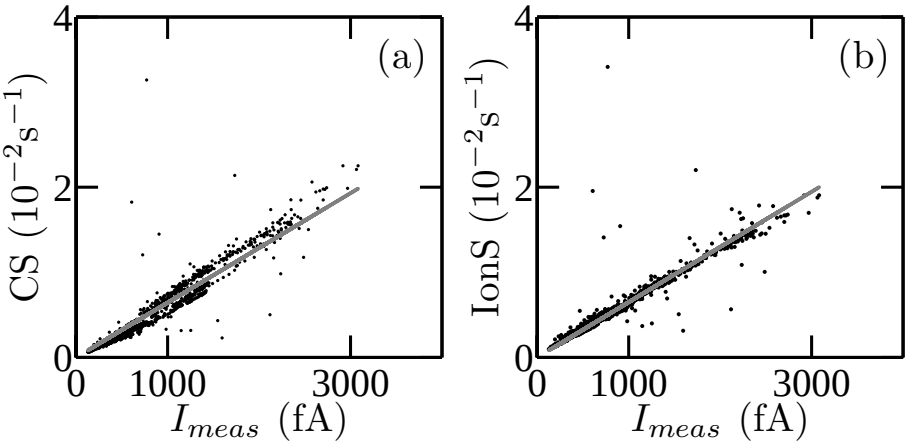

Fig. 5. The values of **(a)** condensation sink and **(b)** ion sink calculated from the DMPS size distributions as a function of the measured ELPI current.

ACPD
9, 15867–15889, 2009

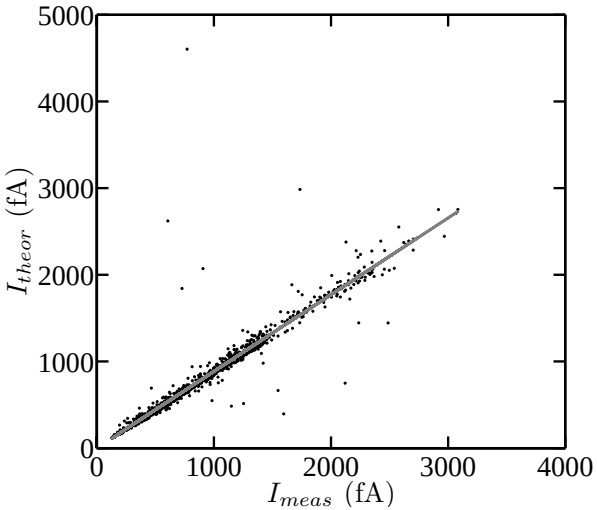

Fig. 6. The theoretical ELPI current as a function of the measured ELPI current. The slope of the fitting is 0.885, which means that the measured current is greater than the theoretical.

ACPD

9, 15867–15889, 2009

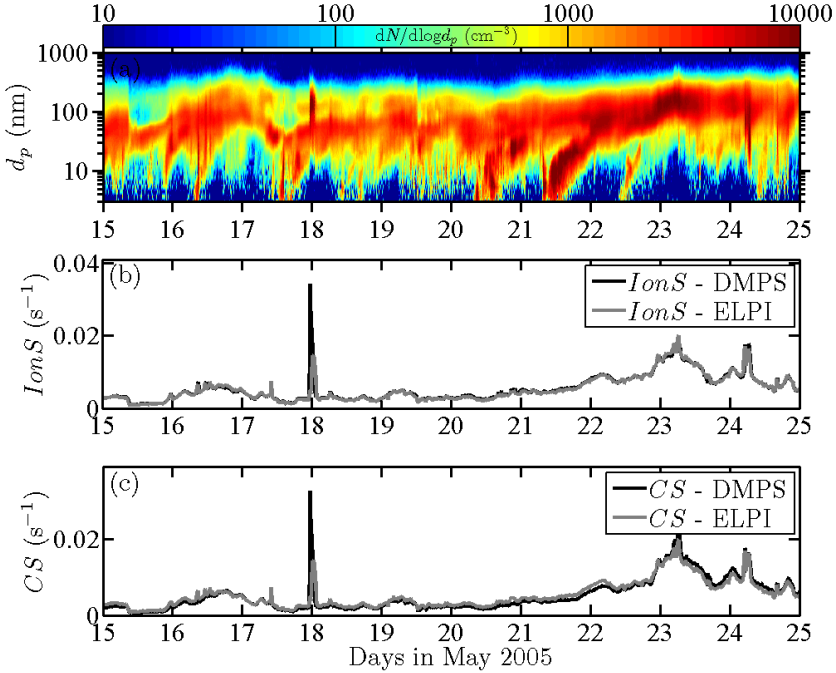

Fig. 7. The number size distributions, ion sink and condensation sink as a function of time. In panels **(b)** and **(c)** there are quantities calculated from the DMPS size distributions and quantities calculated from the ELPI total current using the calibration factors based on the measured ELPI current.